# LIFETIMES OF <sup>26</sup>Al AND <sup>34</sup>Cl IN AN ASTROPHYSICAL PLASMA

Alain Coc, Marie–Geneviève Porquet

Centre de Spectrométrie Nucléaire et de Spectrométrie de Masse, IN2P3-CNRS and Université Paris Sud, 91405 Orsay Campus, France

Frédéric Nowacki

Laboratoire de Physique Théorique de Strasbourg, 3-5 rue de L'Université, 67084 Strasbourg Cedex 2, France

### Abstract

We study here the onset of thermal equilibrium affecting the lifetimes of <sup>26</sup>Al and <sup>34</sup>Cl nuclei within a hot astrophysical photon gas. The <sup>26</sup>Al isotope is of prime interest for gamma ray astronomy with the observation of its delayed  $(t_{\frac{1}{2}}=0.74 \text{ My})$  1.809 MeV gamma–ray line. Its nucleosynthesis is complicated by the presence of a short lived  $(t_{\frac{1}{2}}=6.34 \text{ s})$  spin isomer. A similar configuration is found in <sup>34</sup>Cl where the decay of its isomer (<sup>34m</sup>Cl,  $t_{\frac{1}{2}}=32 \text{ m}$ ) is followed by delayed gamma–ray emission with characteristic energies. The lifetimes of such nuclei are reduced at high temperature by the thermal population of shorter lived levels. However, thermal equilibrium within <sup>26</sup>Al and <sup>34</sup>Cl levels is delayed by the presence of the isomer. We study here the transition to thermal equilibrium where branching ratios for radiative transitions are needed in order to calculate lifetimes. Since some of these very small branching ratios are not known experimentally, we use results of shell model calculations.

PACS numbers: 26.30.+k, 26.20.+f, 21.10.Pc, 23.20.-g

### I. INTRODUCTION

The discovery and the subsequent mapping of <sup>26</sup>Al in the interstellar medium through the detection of its 1809 keV  $\gamma$ -ray line by satellites (HEAO-3, COMPTEL-CGRO, and for the future: INTEGRAL) has increased the interest in <sup>26</sup>Al nucleosynthesis. The potential sites for <sup>26</sup>Al production include supernovae, Wolf-Rayet stars, AGB (Asymptotic Giant Branch) stars and novae (see ref. [1] for a review). Consequently, the nuclear physics involved in <sup>26</sup>Al nucleosynthesis is of renewed importance. Thermonuclear reaction rates involved in <sup>26</sup>Al production and destruction are discussed in a recent compilation [2]. Here we discuss its off-equilibrium destruction rate through the thermal population of excited levels and

in particular of its isomer. If beta decay probabilities are available, lifetimes at thermal equilibrium can be readily calculated. However, thermal equilibrium between the ground and isomeric states are delayed by the large spin difference. This was first studied by Ward and Fowler [3] who set the rule used in <sup>26</sup>Al nucleosynthesis calculations, stating that <sup>26gs</sup>Al and <sup>26m</sup>Al have to be considered either as separate isotopes (no equilibrium) at temperatures below  $\approx 0.4$  GK or as a single one (full equilibrium) above. This temperature is uncomfortably close to the peak temperature attained in nova outbursts ( $\leq 0.35$  GK) or in AGB thermal pulses ( $\leq 0.3$  GK). Moreover, some of the nuclear data used by Ward and Fowler are estimates that are known to be valid only to within many orders of magnitude. Hence, we felt that it was time to reconsider the *onset* of thermal equilibrium in <sup>26</sup>Al. The <sup>26</sup>Al effective lifetime has been calculated [4] using systematics of radiative transition probabilities to evaluate unknown transitions in <sup>26</sup>Al. Here we use instead results of shell model calculations.

The origin for the presence of an isomer in <sup>26</sup>Al is well known. It is an odd-odd nucleus with N = Z (=13). Hence, the two unpaired nucleons are in the same nlj shell  $(j = \frac{5}{2})$ . The most favored configurations are when they couple to  $J^{\pi} = 0^+$  or  $2j^+$  (5<sup>+</sup>) making the ground state (5<sup>+</sup>) and isomer (0<sup>+</sup>). Internal (gamma) transitions from the isomer to the ground state are inhibited by the large spin difference. Beta decay of the isomer (0<sup>+</sup>) to the ground state of the even-even nucleus <sup>26</sup>Mg (0<sup>+</sup>) is not hampered by spin difference and hence constitutes the sole decay mode of <sup>26m</sup>Al ( $t_{\frac{1}{2}}$ =6.34 s). On the contrary the ground state <sup>26gs</sup>Al with  $J^{\pi} = 5^+$  has its beta decay to the <sup>26</sup>Mg ground state forbidden. Hence it decays slowly ( $t_{\frac{1}{2}}$ =0.74 My) towards excited sates of <sup>26</sup>Mg which subsequently de-excite through internal transitions leading to the observed gammas.

A similar configuration occurs in <sup>34</sup>Cl save that the unpaired nucleons belong to a  $j = \frac{3}{2}$ shell, making the situation less contrasted. It has also Z = N (=17), odd-odd, and a relatively long lived isomer. However, contrary to the <sup>26</sup>Al case, the ground state has the lowest spin and hence a shorter half-life (0<sup>+</sup>, 1.53 s) than the isomer (3<sup>+</sup>, 32 m), located 146 keV above. It is also <sup>34m</sup>Cl which decays by beta emission towards excited states of <sup>34</sup>S, and thus emits delayed gammas while <sup>34gs</sup>Cl decays to the <sup>34</sup>S ground state. So on a much shorter time scale, <sup>34</sup>Cl has properties similar to <sup>26</sup>Al when considering the two first levels with high (3<sup>+</sup>;5<sup>+</sup>) and low (0<sup>+</sup>) spins save that there is an inversion in their relative location. The lower spin of <sup>34m</sup>Cl compared to <sup>26m</sup>Al results in a shorter lifetime with respect to beta decay and to a significant decay through internal transition to <sup>34gs</sup>Cl.

Due to its short half life, gamma ray lines resulting from  ${}^{34m}$ Cl decay could only be seen in events where the ambient medium becomes transparent to gamma rays in a matter of hours after the nucleosynthesis phase. This happens in nova outbursts where  ${}^{34}$ Cl has been considered as a source of 511 keV gamma rays [5]. However,  ${}^{34m}$ Cl delayed gamma emission includes also specific lines ( $E_{\gamma} = 2.128$  and 3.304 MeV, with 43% and 12% branching ratio respectively [6] not considered in ref. [5]) which are observationally more interesting. Synthetic gamma ray spectra of novae have been calculated [7,8] including gamma ray emission following the decay of  ${}^{18}$ F whose half–life (110 m) is of the same order of magnitude as for  ${}^{34m}$ Cl (32 m). According to these calculations, gamma rays following  ${}^{18}$ F decay could be detected a few hours after the outburst. In consequence  ${}^{34m}$ Cl should be considered as a potential source of observable gamma ray lines but with a prerequisite study of its modes of production and destruction and in particular its lifetime under astrophysical conditions. For <sup>26</sup>Al and <sup>34</sup>Cl internal transition probabilities, we use experimental data when available or results of shell model calculations otherwise. To check the reliability of these calculations, we first compare theoretical and experimental radiative widths in <sup>26</sup>Al, <sup>34</sup>Cl and neighboring nuclei and deduce confidence limits for the shell model results. Then we calculate the transition to equilibrium with these new values. For this purpose, we consider the first levels as separate nuclides and all possible internal transitions between them together with their beta decays. The set of equations is solved numerically and the results are provided as an analytical fit.

#### II. LIFETIME OF NUCLEI IN A PLASMA

At high densities, lifetimes of nuclei are reduced due to the increasing Fermi energy of the electrons that opens up electron capture channels otherwise energetically forbidden. This effect occurs at densities above  $\rho \approx 10^5$  [9] when the Fermi energy of the electrons,  $[U_F = m_e(((3\pi^2)^{2/3}(\hbar/m_e)^2N_A^{2/3}(Z\rho/A)^{\frac{2}{3}} + 1)^{\frac{1}{2}} - 1)]$  reaches a few tens keV. Here we concentrate on the onset of equilibrium at moderate densities ( $\rho \leq 10^5$ ) that prevail, for instance, in nova outburst. The principles of the calculation are presented in ref. [3] but it is worth while to give here a short summary, taking <sup>26</sup>Al as a typical example.

Equilibration between <sup>26m</sup>Al and <sup>26gs</sup>Al proceeds through intermediate  $E_x \leq 1$  MeV levels [3]. The corresponding two levels (labeled a and b) together with the gamma ray transitions that link them are displayed in Fig. 1. The thick or thin arrows correspond to transition probabilities ( $\lambda_{ij}$ ) that are known experimentally or, respectively, have to be estimated. They are labeled by their electric (*EL*) or magnetic (*ML*) multipolarity (*L*). No arrow links <sup>26m</sup>Al and <sup>26gs</sup>Al since a transition with such a high multipolarity (*M*5) is strongly inhibited even though this rate is slightly enhanced by the photon bath [3]. These two levels are only connected indirectly through transitions via the higher lying levels and in particular those located at  $E_{cm}=0.417$  and 1.058 MeV.

Within stellar environment, the gamma transition probabilities are modified by the thermal photon gas and we use the method exposed in ref. [3]. Let *i* and *j* two levels such that  $E_j > E_i$  and where the only mode of deexcitation for level *j* is a gamma transition to *i*. The evolution of the populations  $(N_j, N_i)$  of these levels is governed by the set of coupled equations [10]:

$$\frac{dN_j}{dt} = -\lambda_{ij}N_j + (-\lambda_{ij}N_j + \lambda_{ji}N_i)u(T)$$
$$\frac{dN_i}{dt} = \lambda_{ij}N_j + (\lambda_{ij}N_j - \lambda_{ji}N_i)u(T)$$

The first term of the second member represents the spontaneous decay  $(j \rightarrow i)$ , the following the stimulated  $(j \rightarrow i)$  and induced  $(i \rightarrow j)$  transitions and u(T) is the photon density:

$$u(T) = \left(\exp\left(\frac{E_j - E_i}{kT}\right) - 1\right)^{-1}$$

The  $\lambda$  coefficients are readily obtained by considering the limits i)  $T \to 0$  where only spontaneous decay occurs, and ii) thermal equilibrium  $(\frac{dN_i}{dt} = 0)$ , that is :

$$i) \quad \hbar \lambda_{ij} = \Gamma_{\gamma;j}$$

$$ii) \quad \frac{\lambda_{ji}}{\lambda_{ij}} = \frac{2J_j + 1}{2J_i + 1} \exp\left(\frac{E_j - E_i}{kT}\right)$$

To be more general, the evolution of the population of the various levels  $(i, j \in \{o, m, a, b, ..\})$  linked by all possible internal gamma transition is represented by a set of linear differential equations which can be written in matrix form as:  $d\mathbf{N}/dt = -\lambda \mathbf{N}$ . This set of equations can be readily solved numerically by using a standard implicit code for nucleosynthesis [4] using the Arnett and Truran [11] prescription. For this purpose, the relevant nuclear levels (o, m, a, b, ..) are introduced as separate "isotopes" connected via "nuclear reactions" (i.e. gamma transitions) whose rates are given by the  $\lambda_{ij}$  matrix elements. To these "reactions", one must add beta decay rates from the various levels to the daughter nucleus. When not available experimentally (i.e. for levels above the ground and isomeric states) these beta decay rates are obtained from shell model calculations [12]. (At  $\rho \gtrsim 10^5$ , one must take into account that  $\log(ft)$  depends on the electronic density and hence on  $\rho$  [9]. This is not considered here where we limit ourselves to *low* densities.) Then, starting with initial abundance such that only the ground or isomeric state are populated one can obtain their lifetime by calculating numerically the time needed for the initial abundance to be reduced by a 1/e factor.

#### III. AVAILABLE NUCLEAR DATA

In <sup>26</sup>Al, the known transitions linking the 3<sup>+</sup> level with the ground state and the 1<sup>+</sup> level with the isomer, are an E2, and a M1, respectively (Fig. 1). However, the possibility remains of a M3 transition linking the 3<sup>+</sup> and isomeric levels and of an E2 between the 1<sup>+</sup> and 3<sup>+</sup> levels [3]. Even though the branching ratios M3/E2 and E2/M1 are expected to be very small, they provide the links between the ground state and isomer but delay the onset of equilibrium. These branching ratios are too small to be measured and accordingly, Ward and Fowler [3] had to estimate them. They assumed one Weisskopf *unit* (W.u.) for electric transitions (EL) or one Moszkowski *unit* (M.u.) for magnetic ones (ML). However, the value of 1. M.u/1. W.u. they used for the  $M3(a \rightarrow m)/E2(a \rightarrow o)$  lies well outside the range (7 orders of magnitude [4,13]) spanned by experimental values. Indeed, the  $a \rightarrow o$  transition has been measured and corresponds to 7.7 W.u., this is equivalent to assume 7.7 M.u. for the  $a \rightarrow m$  transition which is above the upper limit  $\approx 1$  M.u. derived from statistics of experimental values of M3 transition probabilities [13]. For the other branching ratio (E2/M1), the choice of 1 W.u./1 M.u. is compatible with the M1 experimental value of 2.4 M.u. and the wide range of E2 reduced transition strengths [14] ( $\approx 10^{-2}-10^2$  W.u).

In <sup>34</sup>Cl, contrary to the <sup>26</sup>Al case, an internal  $(M3, m \rightarrow o)$  transition links the isomer to the ground state with a 44.6% branching ratio (Fig. 2). The two 1<sup>+</sup> levels (*a* and *b* at 0.461 and 0.666 MeV) decay to the ground state with known probabilities [15,6]. Only upper limits for the branching ratios are available for the transition to the isomer  $(M1, a \rightarrow m \text{ and} b \rightarrow m)$  or between the two 1<sup>+</sup> levels  $(M1 + E2, b \rightarrow a)$ . The next level (2<sup>+</sup>) is located at 1.230 MeV and has known radiative transition probabilities to all the <sup>34</sup>Cl levels below save for the ground state where only an upper limit is available. These upper limits are well above those provided by statistics of radiative reduced transition strengths [14]. They only reflect experimental limitations and accordingly have not been considered in our calculations. As for the <sup>26</sup>Al case, experimentally known transitions are represented by thick arrows (Fig. 2) while thin arrows represent missing data that have to be obtained theoretically.

#### **IV. SHELL MODEL CALCULATIONS**

Instead of using *one* Weisskopf or Moszkowski *unit* as estimates of radiative transition probabilities, we use shell model calculations to provide the unknown ones. We also compare calculated and experimental values in the neighboring nuclei in order to estimate confidence limits for the shell model results.

The calculations include the full sd shell  $(d_{\frac{5}{2}}, s_{\frac{1}{2}} \text{ and } d_{\frac{3}{2}} \text{ orbitals})$  for protons and neutrons. Here we use the USD interaction of Wildenthal [16]. We have also done calculations with the two sets of the Chung-Wildenthal (CW) [17] interaction (lower and upper sd part) in order to compare with USD results. Indeed, the USD interaction is designed for the full A=16-40 mass range and therefore should provide the most reliable values but comparison with CW calculations allows to appreciate the uncertainties involved in such calculations. The diagonalization procedure and transition calculations are performed using the shell model code Antoine [18,19]. For the calculations of electromagnetic transitions, we have used a polarization effective charge of 0.5, and the following gyromagnetic factors,  $g_s(p) =-5.59$ ,  $g_l(p) =1.0$ ,  $g_s(n) =3.83$  and  $g_l(n) =0$ .

All the transition probabilities calculated for <sup>26</sup>Al, its odd-A neighbors (<sup>25</sup>Al and <sup>25</sup>Mg), <sup>34</sup>Cl and its odd-A neighbours (<sup>33</sup>Cl and <sup>33</sup>S) are given in Tables I to III in comparison with the experimental values. Fig. 3 shows that most of the calculated radiative widths lie within a factor of three from the experimental values. Accordingly, the upper and lower limits of the transition probabilities used in the present calculations are obtained by multiplying the theoretical values by a factor of 3 and 1/3 respectively.

## V. RESULTS FOR <sup>26</sup>Al AND <sup>34</sup>Cl EFFECTIVE LIFETIMES

To calculate <sup>26</sup>Al and <sup>34</sup>Cl lifetimes we use experimental or theoretical data (Table I, II and III) as discussed in the preceding sections following the method exposed in the second section. We emphasize that by numerically solving the set of coupled differential equations representing all the transitions ( $\gamma$  and  $\beta$ ) displayed in Fig. 1 and Fig. 2 we make no assumption, at any stage, on the degree of equilibrium achieved. Accordingly, the main decay channel (e.g. internal transition or  $\beta$  decay from the *a* level in <sup>26</sup>Al) is the result of the calculation.

### **A.** <sup>26</sup>**Al**

With this method, Coc and Porquet [4] have already compared the two formulas [3,20] giving the <sup>26gs</sup>Al off–equilibrium effective lifetime. Ward and Fowler [3] assumed that in

these condition <sup>26</sup>Al decays to <sup>26</sup>Mg predominantly through the beta decay of the 3<sup>+</sup> (a) level while Vogelaar [20] favors the decay from the 0<sup>+</sup> (m) level. When the calculations are made numerically, without *a priori* assumptions, the only significant decay channel [4] is the one assumed by Vogelaar [20] i.e. through internal transition to the isomer followed by its beta decay. Only in the extreme case, where the  $M3(a \rightarrow m)$  transition probability is assumed to be around  $10^{-3}$  M.u. does beta decay from the 3<sup>+</sup> level become significant as the transition to the 0<sup>+</sup> level is strongly inhibited. This very small value corresponds to the lower limit deduced from the statistics of M3 reduced strength [13] but can be rejected on the basis of shell model calculations ( $\approx 1$  M.u.).

Using now the updated nuclear data, the <sup>26</sup>Al effective life time is depicted in Fig. 4 by a solid line. (For comparison, the dash-dotted line represents the result of the Ward and Fowler [3] off-equilibrium formula.) The hatched area represents the uncertainty due to the confidence limits assigned to the shell model calculations as discussed above. The resulting uncertainty is too small to have any consequence in astrophysics. Below  $\approx 0.15$  GK, the lifetime is equal to its laboratory value. Above  $\approx 0.4$  GK it is equal to its equilibrium value  $\lambda_{eq} = 9.9 \times 10^{-3} \exp\left(\frac{-2.651}{T_9}\right)$  [3] represented by a dashed curve. Below, it can be approximated (dashed curve) by using the following formula which gives the transition probability (i.e. the inverse of the effective lifetime)

$$\lambda_{off} = 2.97 \times 10^{-14} + 4.07 \times 10^{-2} \exp\left(\frac{-4.839}{T_9}\right) + 2.10 \times 10^8 \exp\left(\frac{-12.28}{T_9}\right)$$

Here, as usual in astrophysics,  $T_9$  represents the temperature in units of GK (10<sup>9</sup> K). The first term corresponds to the  ${}^{26gs}$ Al laboratory decay. The two last terms originate from the population of the 3<sup>+</sup> level,  $\left(\frac{2J_o+1}{2J_a+1}\exp\left(-\frac{E_a}{KT}\right)\right)$  times the probability that it decays to the isomeric level ( $\lambda_{ma}$ ) or that it undergoes an induced transition to the 1<sup>+</sup> level  $\left(\lambda_{ba} \equiv \lambda_{ab} \frac{2J_b+1}{2J_a+1}\exp\left(-\frac{E_b-E_a}{KT}\right)\right)$ . As shown in Fig. 4, the two dashed curves representing the equilibrium and off-equilibrium lifetimes meet around 0.4 GK. Hence, as suggested in ref. [4], the temperature below which  ${}^{26gs}$ Al and  ${}^{26m}$ Al have to be considered as separate nucleides is not affected by the use of new data.

### **B.** <sup>34</sup>Cl

Figure 5 displays the effective <sup>34</sup>Cl lifetime as a function of temperature with the same convention as for <sup>26</sup>Al in Fig. 4. The transition between the laboratory lifetime to the equilibrium lifetime occurs between 0.12 and 0.25 GK and the remaining nuclear uncertainties have a negigible effect (dashed area). The decay rate at equilibrium is given by:

$$\lambda_{eq} = \frac{0.454 + 1.40 \times 10^{-3} \exp\left(\frac{-1.699}{T_9}\right)}{1 + 7 \exp\left(\frac{-1.699}{T_9}\right)}$$

Contrary to the <sup>26</sup>Al case, at equilibrium, the lifetime increases with temperature following the thermal depopulation of the short lived ground state. At lower temperature, <sup>34m</sup>Cl and <sup>34gs</sup>Cl have to be considered separately and the <sup>34m</sup>Cl decay rate is approximated by:

$$\lambda_{off} = 3.61 \times 10^{-4} + 8.77 \times 10^6 \exp\left(\frac{-3.651}{T_9}\right)$$

The results obtained with these formula are represented by dashed lines on Fig. 5. They meet at  $T \approx 0.22$  GK which marks the limit for equilibrium. This last formula approximates very well the result of the numerical calculation. Since it includes only the effect of the  $m \rightarrow a$  transition, it shows that only this transition has a significant influence on <sup>34m</sup>Cl lifetime.

#### VI. CONCLUSIONS

We calculated by numerical integration of the coupled differential equations the lifetimes of <sup>26</sup>Al and <sup>34</sup>Cl in a hot astrophysical photon gas assuming *low* densities ( $\leq 10^5$  g/cm<sup>3</sup>). We obtained crucial radiative transition probabilities, not available experimentally, from shell model calculations. The temperature (0.4 GK) which limits the domain where <sup>26gs</sup>Al and <sup>26m</sup>Al have to be considered separately is insensitive to the remaining nuclear uncertainties. Below this temperature and down to  $\approx 0.16$  GK, the <sup>26gs</sup>Al lifetime is shorter (by up to four orders of magnitude) than the one proposed by Ward and Fowler. The discrepancy comes from their hypothesis on the main <sup>26</sup>Al decay channel (beta decay from the 3<sup>+</sup> level) which is not correct as pointed out by Vogelaar. Below 0.22 GK, <sup>34gs</sup>Cl and <sup>34m</sup>Cl are not at equilibrium and have to be treated as two separate nuclides. The <sup>34</sup>Cl lifetime drops rapidly above 0.15 GK (two orders of magitudes between 0.15 and 0.2 GK). We provide analytical formulas that approximate the <sup>26gs</sup>Al and <sup>34m</sup>Cl lifetimes when they are not yet in equilibrium with <sup>26m</sup>Al and <sup>34gs</sup>Cl respectively.

Considering the various <sup>26</sup>Al potential astrophysical sources (i.e. temperature and density conditions), it is not clear whether this modified lifetime will affect significantly its production. On the contrary <sup>34</sup>Cl is only of interest for novae and only the hottest ones can synthetize isotopes in the S–Ar region. Unfortunately, our calculations show that in the conditions that prevail in such events (up to  $\approx 0.35$  GK), <sup>34m</sup>Cl is efficiently destroyed by induced transition to the short–lived <sup>34gs</sup>Cl.

### VII. ACKNOWLEDGMENTS

We are grateful to E. Caurier, H.T. Duong, B. Roussière and D. Lunney for valuable discussions. This work was partially supported by PICS 319.

### FIGURES

FIG. 1. Level scheme for <sup>26</sup>Al. The first levels of <sup>26</sup>Al with their characteristics are represented together with the beta and gamma transitions considered in the calculations. The thick arrows represent the experimentally known transitions while the thin ones come from shell model calculations. The matrix element  $\lambda_{ij}$  represents the transition probability from level j to level i.

FIG. 2. Level scheme for <sup>34</sup>Cl. Conventions are the same as Fig. 1 (see Tables for details.)

FIG. 3. Comparison between experimental and theoretical gamma widths. Most calculated widths deviate from experimental data by less than a factor of three (dashed lines.)

FIG. 4. The effective lifetime of <sup>26</sup>Al as a function of temperature calculated using shell model transition probabilities (solid line). The hatched area shows the corresponding uncertainty (see text.) The analytic formulas for  $\lambda_{off}$  and  $\lambda_{eq}$  reproduce the effective lifetime (dashed curves) on both sides of the equilibrium temperature. The dash-dotted curve corresponds to the formula provided by Ward and Fowler [3]

FIG. 5. Effective lifetime of  $^{34m}$ Cl as a function of temperature. (Same conventions as in Fig. 4.)

### REFERENCES

- [1] N. Prantzos and R. Diehl, *Phys. Rep.* **267**, 1 (1996).
- [2] C. Angulo et al., (The NACRE collaboration), Nucl. Phys. A656, 3 (1999).
- [3] R.A. Ward and W.A. Fowler, *Astrophys. J.* **238**, 266 (1980).
- [4] A. Coc and M.-G. Porquet, Proceedings of the Tours Symposium on Nuclear Physics III, AIP Conference Proceedings 425, 457 (1998).
- [5] M.D. Leising and D.D. Clayton, Astrophys. J. **323**, 159 (1987).
- [6] P.M. Endt, Nucl. Phys. A521, 1 (1990).
- [7] J. Gómez–Gomar, M. Hernanz, J. José and J. Isern, MNRAS **296**, 913 (1998).
- [8] M. Hernanz, J. José, A. Coc, J. Gómez-Gomar and J. Isern, to appear in Astrophys. J. Letters, astro-ph/9910111 prepint, (1999).
- [9] G.M. Fuller, W.A. Fowler and M.J. Newman, Astrophys. J. Sup. 42, 447 (1980).
- [10] C. Cohen-Tannoudji, J. Dupont-Roc, and G. Grynberg, Processus d'interaction entre photons et atomes, Paris, InterEditions/Editions du CNRS, 1988, ch 4, p. 249. or A. Kastler, Optique, Paris, Masson & C<sup>ie</sup>, 1965, ch 36, p. 949 for instance.
- [11] W.D. Arnett and J.W. Truran, Astrophys. J. 157, 339 (1969).
- [12] T. Kajino, E. Shiino, H. Toki, B.A. Brown and B.H. Wildenthal, Nucl. Phys. A480, 175 (1988).
- [13] B. Roussière et al., Nucl. Phys. A643, 331 (1998).
- [14] P.M. Endt, Atomic Data and Nuclear Data Tables 23, 3 (1979).
- [15] Table of Isotopes, seventh edition, edited by C.M. Lederer and V.S. Shirley, John Wiley & Sons, New York, 1978.
- [16] B. H. Wildenthal, Prog. Part. Nucl. Phys. **11**, 5 (1984).
- [17] W. Chung, Ph. D. Thesis, Mich. State Univ., East Lansing (1976).
- [18] E. Caurier, code Antoine Strasbourg (1989)
- [19] E. Caurier and F. Nowacki, Act. Phys. Pol. **B30**, 705 (1999).
- [20] R.B. Vogelaar, Ph. D. Thesis, California Institute of Technology (1989).

# TABLES

Nuclei	Transition	$t_{\frac{1}{2}}$	$E_{\gamma}$	$\gamma$ –branching	B(M3)	B(M3)
		2		ratio	Exp.	USD
			(MeV)		$(\mu_N^2 \; fm^4)$	$(\mu_N^2 \ fm^4)$
<sup>24</sup> Na	$0.472;1^+ \rightarrow 0;4^+$	$20.2{\pm}0.07~\mathrm{ms}$	0.472	0.9995	$1046 \pm 4$	1795.
$^{24}Al$	$0.426;1^+ \rightarrow 0;4^+$	$131.3{\pm}2.5~\mathrm{ms}$	0.426	0.82	$270{\pm}12$	725.
$^{26}$ Al	$0.417; 3^+ \rightarrow 0.228; 0^+$	$1.25{\pm}0.03~\mathrm{ns}$	0.189	unknown	—	1206.
$^{34}Cl$	$0.146; 3^+ \rightarrow 0; 0^+$	$32.00{\pm}0.04~{\rm m}$	0.146	0.381	$15.2{\pm}0.2$	18.0
$^{38}\mathrm{Cl}$	$0.671; 5^- \rightarrow 0; 2^-$	$715\pm3~\mathrm{ms}$	0.671	1.	$2.52{\pm}0.01$	0.008

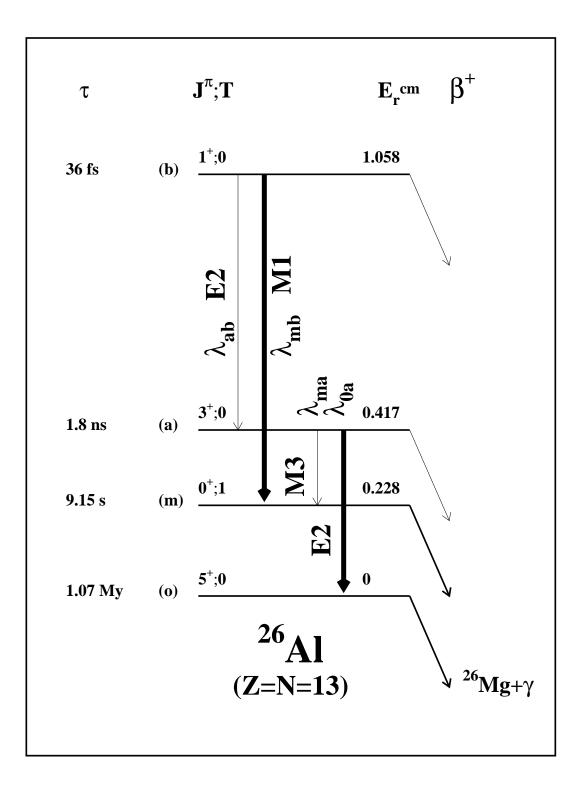
TABLE I. Comparison of M3 transitions

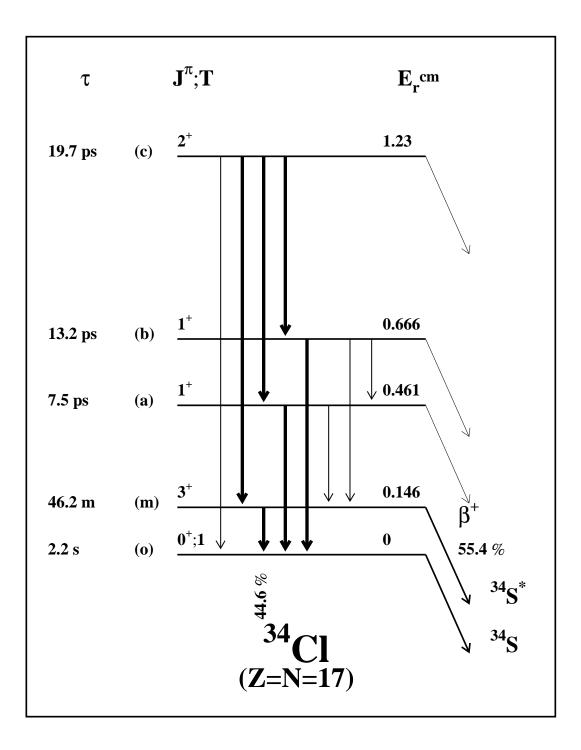
TABLE II. Comparison of E2 transitions

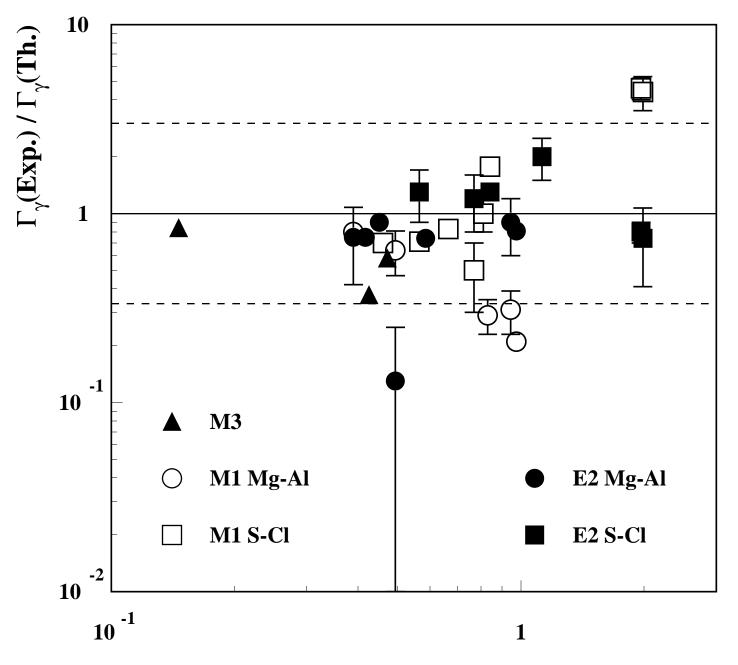
Nuclei	Transition	$t_{\frac{1}{2}}$	$E_{\gamma}$	B(E2)	B(E2)
		2		Exp.	USD
			(MeV)	$(e^2 fm^4)$	$(e^2 \ fm^4)$
$^{25}Mg$	$0.585; 1/2^+ \rightarrow 0; 5/2^+$	$3.38{\pm}0.05~\mathrm{ns}$	0.585	$2.44\pm0.04$	33.3
$^{25}Mg$	$0.975; 3/2^+ \rightarrow 0; 5/2^+$	$11.3{\pm}0.3~\mathrm{ps}$	0.975	$3.5\pm0.3$	4.3
$^{25}Mg$	$0.975; 3/2^+ \rightarrow 0.585; 1/2^+$	$11.3{\pm}0.3~\mathrm{ps}$	0.390	$49\pm22$	65
$^{25}Al$	$0.452; 1/2^+ \rightarrow 0; 5/2^+$	$2.29{\pm}0.03~\mathrm{ns}$	0.452	$13.2\pm0.2$	14.6
$^{25}Al$	$0.945; 3/2^+ \rightarrow 0; 5/2^+$	$4.3 \pm 1.1 \text{ ps}$	0.945	$8\pm3$	8.6
$^{25}Al$	$0.945; 3/2^+ \rightarrow 0.452; 1/2^+$	$4.3 \pm 1.1 \text{ ps}$	0.493	$10 \pm 10$	74.6
$^{26}Al$	$0.417; 3^+ \rightarrow 0; 5^+$	$1.25{\pm}0.3~\mathrm{ns}$	0.417	$36\pm1$	48.
$^{26}Al$	$1.058; 1^+ \rightarrow 0.417; 3^+$	$25\pm5$ fs	0.641	unknown	5.8
<sup>33</sup> Cl	$1.986; 5/2^+ \rightarrow 0; 3/2^+$	$55{\pm}11$ fs	1.986	$49{\pm}22$	65
$^{33}\mathrm{Cl}$	$1.986; 5/2^+ \rightarrow 0.811; 3/2^+$	$55{\pm}11$ fs	1.176	<133	25
$^{33}S$	$0.841; 1/2^+ \rightarrow 0; 3/2^+$	$1.17{\pm}0.03~\mathrm{ps}$	0.841	$26.4{\pm}1.5$	20
$^{33}S$	$1.967; 5/2^+ \rightarrow 0; 3/2^+$	$104{\pm}14$ fs	1.967	$44{\pm}7$	55
$^{33}S$	$1.967; 5/2^+ \rightarrow 0.841; 1/2^+$	$104{\pm}14$ fs	1.126	$39{\pm}10$	19
$^{34}\mathrm{Cl}$	$0.461; 1^+ \rightarrow 0.146; 3^+$	$5.2 \pm 0.3$ ps	0.315	<178.	5.44
$^{34}\mathrm{Cl}$	$0.666; 1^+ \rightarrow 0.461; 1^+$	$9.1{\pm}0.6$ ps	0.205	<1724.	20.8
$^{34}\mathrm{Cl}$	$0.666; 1^+ \rightarrow 0.146; 3^+$	$9.1{\pm}0.6$ ps	0.519	<16.6	18.5
$^{34}\mathrm{Cl}$	$1.230; 2^+ \rightarrow 0.661; 1^+$	$13.7 \pm 0.9 \text{ ps}$	0.565	$33{\pm}11$	24.9
$^{34}\mathrm{Cl}$	$1.230; 2^+ \rightarrow 0.461; 1^+$	$13.7{\pm}0.9~\mathrm{ps}$	0.769	$32 \pm 11$	25.7
$^{34}\mathrm{Cl}$	$1.230; 2^+ \rightarrow 0.146; 3^+$	$13.7{\pm}0.9~\mathrm{ps}$	1.084	$4.2 \pm 3.1$	0.621
$^{34}\mathrm{Cl}$	$1.230; 2^+ \rightarrow 0; 0^+$	$13.7{\pm}0.9~\mathrm{ps}$	1.230	< 0.074	0.221

Nuclei	Transition	$t_{\frac{1}{2}}$	$E_{\gamma}$	B(M1)	B(M1)
		2		Exp.	USD
			(MeV)	$(\mu_N^2)$	$(\mu_N^2)$
$^{25}Mg$	$0.975; 3/2^+ \rightarrow 0; 5/2^+$	$11.3 \pm 0.3 \text{ ps}$	0.975	$(2.8 \pm 0.1) \times 10^{-2}$	0.035
$^{25}Mg$	$0.975; 3/2^+ \rightarrow 0.585; 1/2^+$	$11.3{\pm}0.3~\mathrm{ps}$	0.390	$(1.69 \pm 0.06) \times 10^{-3}$	0.008
$^{25}Al$	$0.945; 3/2^+ \rightarrow 0; 5/2^+$	$4.3\pm1.1$ ps	0.945	$(4.3 \pm 1.2) \times 10^{-3}$	0.13
$^{25}Al$	$0.945; 3/2^+ \rightarrow 0.452; 1/2^+$	$4.3{\pm}1.1~\mathrm{ps}$	0.493	$(4.2 \pm 1.1) \times 10^{-2}$	0.066
<sup>26</sup> Al	$1.058;1^+ \rightarrow 0.228;0^+$	$25\pm5$ fs	0.829	$2.76 {\pm} 0.55$	9.7
<sup>33</sup> Cl	$0.811; 1/2^+ \rightarrow 0; 3/2^+$	$1.2{\pm}0.2$ ps	0.811	$(6.2\pm1.0)\times10^{-2}$	0.063
$^{33}\mathrm{Cl}$	$1.986; 5/2^+ \rightarrow 0; 3/2^+$	$55{\pm}11$ fs	1.986	$(7.6\pm1.6)\times10^{-2}$	0.017
$^{33}S$	$0.841; 1/2^+ \rightarrow 0; 3/2^+$	$1.17{\pm}0.03~\mathrm{ps}$	0.841	$(5.5\pm0.2)\times10^{-2}$	0.031
$^{33}S$	$1.967; 5/2^+ \rightarrow 0; 3/2^+$	$104{\pm}14$ fs	1.967	$(3.7\pm0.5)\times10^{-2}$	0.008
<sup>34</sup> Cl	$1.230; 2^+ \rightarrow 0.666; 1^+$	$13.7{\pm}0.9~\mathrm{ps}$	0.565	$(5.0\pm0.5)\times10^{-3}$	0.0072
$^{34}\mathrm{Cl}$	$1.230; 2^+ \rightarrow 0.461; 1^+$	$13.7{\pm}0.9~\mathrm{ps}$	0.769	$(8.8 \pm 4.5) \times 10^{-4}$	0.0025
$^{34}\mathrm{Cl}$	$1.230; 2^+ \rightarrow 0.146; 3^+$	$13.7{\pm}0.9~\mathrm{ps}$	1.084	$(3.2 \pm 2.5) \times 10^{-4}$	0.0016
$^{34}\mathrm{Cl}$	$0.666; 1^+ \rightarrow 0.461; 1^+$	$9.1{\pm}0.6~\mathrm{ps}$	0.205	< 0.005	0.0007
$^{34}\mathrm{Cl}$	$0.666; 1^+ \rightarrow 0; 0^+$	$9.1{\pm}0.6~\mathrm{ps}$	0.666	$(1.47 \pm 0.10) \times 10^{-2}$	0.018
$^{34}\mathrm{Cl}$	$0.461; 1^+ \rightarrow 0; 0^+$	$5.2{\pm}0.3$ ps	0.461	$(7.74 \pm 4.6) \times 10^{-2}$	0.110

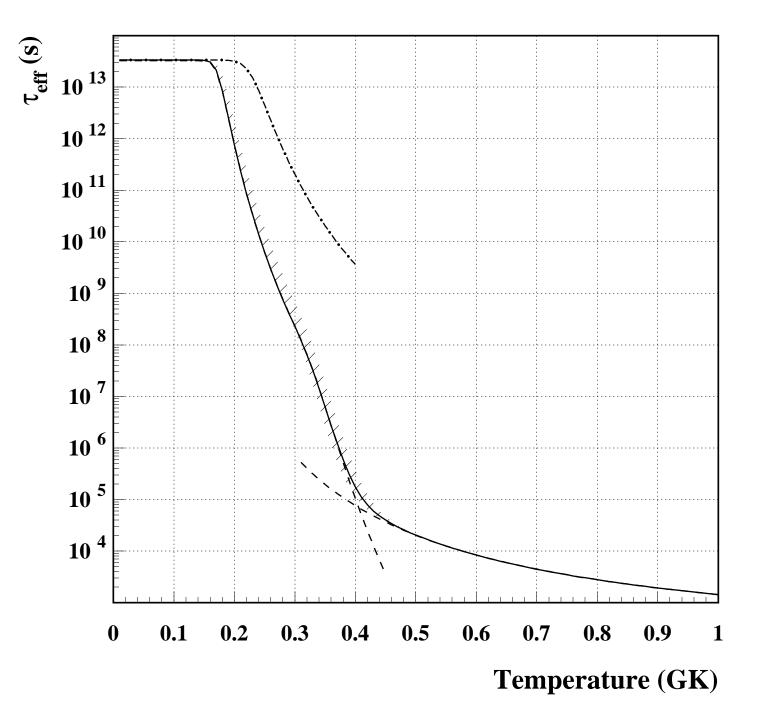
TABLE III. Comparison of M1 transitions

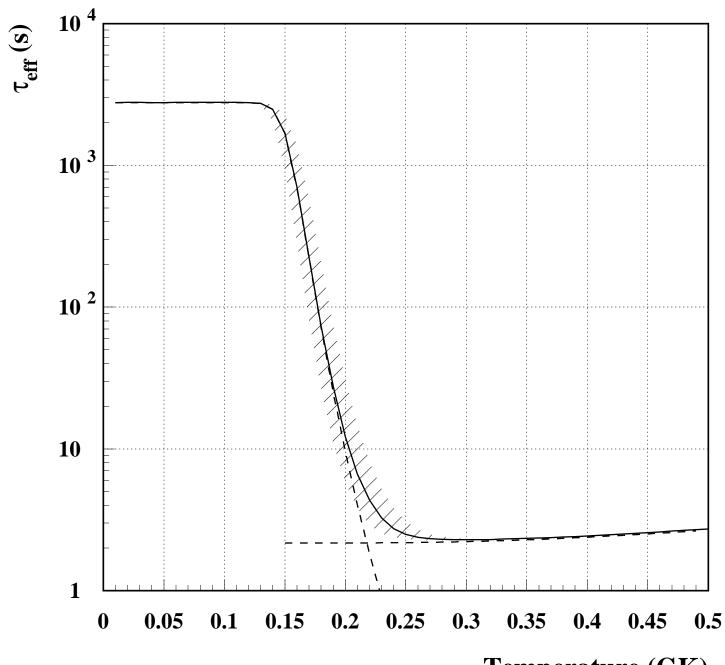






 $E_{\gamma}$  (MeV)





**Temperature (GK)**